JOURNAL OF MATERIALS SCIENCE **35** (2000) 4405–4414

Crystallisation of PET with strain, strain rate and temperature

J. O. FERNANDEZ, G. M. SWALLOWE*
Department of Physics, Loughborough University, Loughborough, Leics., LE11 3TU, UK
E-mail: G.M.SWALLOWE@LBORO.AC.UK

The mechanical properties of Poly ethylene terephthalate (PET) were studied over several decades of strain rate and a temperature range of 263 K–453 K. Tests were carried out in the range 10^{-3}–10^{4} s^{-1} using a conventional Hounsfield machine and two high strain rate test systems. Strain limited tests were carried out at all the strain rates and the temperature rises were estimated from the area under the stress strain curves. X-ray diffraction was used to extract interatomic plane distances and crystallite dimensions. Differential Scanning Calorimetry (DSC) was employed to estimate the degree of crystallinity of the material and the kinetics of crystallisation. PET yield stress increased with strain rate with a sharp increase at rates of 10^{3} s^{-1} and above. It crystallised into the triclinic form at rates above 10^{3} s^{-1} beyond 140% strain but crystallisation was not observed at lower strain rates. Increases of up to 40% in crystallinity content were found which, it is concluded, were thermally induced after the test ended. The results shed light on the development of crystallinity in PET as a function of strain, strain rate and temperature and indicate that the rapid increase in yield and flow stresses previously reported cannot be accounted for by increases in crystallinity.

1. Introduction

The use of the polyester Polyethylene Terephthalate (PET) as a consumer fibre dates back to 1953. It is also widely used in the beverage bottle and food packaging industry due to its high strength, toughness and good resistance to chemicals and grease. The PET repeat unit consists of one benzene ring, two ethers, two carbonyl groups and two methylene units. The crystal structure of PET is triclinic with one chemical unit per cell [1]. The *d* spacing for the most commonly observed x-ray diffraction peaks are 5.11, 4.04 and 3.46 Å corresponding to planes with Miller indexes (010), (110) and (100) [2]. It undergoes the glass transition at about 343 K and melts at approximately 533 K. It has been reported that during cold drawing at low rates the molecular chains first orient in the direction of the stress and that this is followed by crystallisation, [2–4]. This is called strain induced crystallisation as opposed to thermally induced crystallisation. It has also been reported that the crystal size increases with annealing temperature. PET undergoes cold crystallisation on heating from the glass [5] as a result of the heat induced movement of chains which results in a transition into a thermodynamically more stable state. Two melting peaks, a minor one at low temperature and a major one at higher temperature, may be detected after annealing PET, [6]. Blundell and Osborn [7] proposed that the minor melting point was associated with the melting of the crystallites formed during the previous crystallisation process and the large melting peak at higher temperatures was due to melting and recrystallisation into more perfect crystals during the heating run. Muller *et al*. [8] argued that, although the reorganisation process is not seen in the thermogram, it nonetheless occurs. On the other hand, the two melting peaks may be due to the melting of crystalline entities of different size and/or degree of perfection, [9, 10].

Semi crystalline polymers have been observed to show slow increases in yield stress and flow stress with increasing strain rate at strain rates of up to 10^{2} s^{-1} and rapid increases in flow stresses at higher rates [11]. Work on PEK and PEEK has shown an association between this rapid flow stress increase and crystallinity increases in the polymer [12] and preliminary results on PET also showed an association between rapid flow stress increases and dramatic increases in crystallinity [13]. The observed flow stress increases cannot be explained on the basis of the Eyring formulation and these authors have speculated that the crystallinity increases may offer an explanation for the extremely rapid flow stress increases. Time resolved X-ray work carried out at rather lower strain rates ($\sim$10 s^{-1}) [14] have indicated that the crystallinity increases observed in the drawing of PET occur mainly after the drawing process has finished. However rapid flow stress increases are not observed at these low strain rates and the very rapid deformation and adiabatic nature of high rate tests may give rise to rapid crystallinity increases by another mechanism.

* Author to whom correspondence should be addressed.

The morphology of PET, and changes in the morphology after tensile experiments at low strain rates, have been well described. However, the microstructure of PET after high strain rate tests has been scarcely mentioned and topological studies are lacking. The purpose of the work described in this paper is to provide information about the performance of PET over several decades of strain rate in compression with particular emphasis on high rates, and to study the morphological changes under various mechanical and thermal conditions. The study is not only of interest in its own right but sheds light on the relationship between the process of strain induced crystallisation and rapid flow stress increases.

2. Experimental

Samples were machined into cylinders of approximate dimensions 4 mm diameter by 2 mm height from ICI grade B73 PET plaque. The samples were preconditioned to chosen temperatures in the range 263 K to 453 K by heating to the desired temperature for 30 minutes before a test and the compression tests were then carried out at the chosen temperature. X-ray diffraction scans were taken at room temperature on samples recovered after mechanical testing when the samples reached ambient conditions and the compression ended. Thermal analysis was carried out after the X-ray diffraction.

2.1. Mechanical tests

Compressive tests were carried out using a conventional Hounsfield tensile-compressive test machine and two high strain rate machines, namely a Dropweight and a Cross Bow system. The high rate test systems are extensively described elsewhere [12, 15]. Strain limited tests were carried out by halting the compression by means of metal rings. The internal diameters of the rings were chosen so that they would be greater than the sample diameter at the end of the test. The thickness of the rings were 1.5, 1, 0.5 and 0.31 mm. Thus, for specimens 2 mm thick, the strains attained were around 30, 70, 140 and 185%. The purposes of the strain limited tests were to study the influence of strain in the deformation process by stopping sample strain at specified levels. The temperature rise at a given strain was estimated from the stress-strain curves using the expression:

$$\Delta T = \frac{\int \sigma \, \mathrm{d}\varepsilon}{\rho C_{\mathrm{P}}} \tag{1}$$

where σ is the stress, ε the strain, ρ is the density approximately equal to 1.35 g cm^{-3}, and C_{P} the specific heat equal to 1.315 J g^{-1} K^{-1}. Integration of the curves was carried out from the start of the stress-strain curve to the chosen value of strain in order to determine the temperature rise at that strain. This equation assumes that the change in internal energy is zero, i.e., all the work is transformed into heat.

2.2. X-ray diffraction

X-ray diffraction patterns were obtained using a Philips PW1050/25 diffractometer running at 40 kV and 20 mA in reflection mode. A nickel filter was used to select the copper K_α peak. The system was calibrated using a silicon sample. The difference between the silicon standard experimental results and the International Tables of Powder Diffraction was less than 0.002 Å for all observed peaks.

The size of crystallites in a direction perpendicular to the family $(hk\ell)$can be estimated using Scherrer's equation:

$$L_{hk\ell} = \frac{\lambda}{\beta \cos\theta} \tag{2}$$

where β is the width at half maximum in radians and θ the Bragg angle. The method followed to fit the peaks was similar to that of Cakmak and Kim [16]. Three different samples were used to obtain the values of d-spacing and crystal size at each thermomechanical condition.

2.3. Thermal analysis

Thermal analysis was carried out in a Mettler DSC30 measuring cell connected to a Mettler TC10A processor. The system was subjected to heat flow and temperature calibration using standard materials. DSC was performed on approximately 10 mg samples in an argon atmosphere at 10 K min^{-1}. The data values are the average of six scans. The degree of crystallinity was calculated using the expression:

$$\chi_{\mathrm{C}} = \frac{\Delta H}{\Delta H_{\mathrm{m}}^{\mathrm{o}}} \tag{3}$$

where ΔH is the measured heat of fusion and $\Delta H_{\mathrm{m}}^{\mathrm{o}}$ is the heat of fusion of 100% crystalline PET equal to 115 J g^{-1} [17]. The kinetics analysis of crystallisation was carried out in the DSC by varying the scanning rate between 1 and 20 K min^{-1}. The equation of differential methods can be written as:

$$\frac{\mathrm{d}\alpha}{\mathrm{d}t} = kg(\alpha) \tag{4}$$

The activation energy for crystallisation was estimated following the Kissinger [18] and Ozawa [19] methods. Both methods are based on the dependence of the transformation peak position on the heating rate. In the case of this work, the peak observed was the cold crystallisation peak. Kissinger reported that:

$$\frac{\mathrm{d}\left(\mathrm{Ln}\frac{\phi}{T_{\mathrm{m}}^2}\right)}{\mathrm{d}\left(\frac{1}{T}\right)} = -\frac{E}{R} \tag{5}$$

whereas Ozawa suggested that:

$$\frac{\mathrm{d}(\log\phi)}{\mathrm{d}\left(\frac{1}{T}\right)} = -0.457\frac{E}{R} \tag{6}$$

where ϕ is the heating rate and R the gas constant. The pre-exponential factor can be calculated using Rogers

and Smith formula, [20]:

$$A = \frac{\phi E\, e^{\frac{E}{RT_{\max}}}}{RT_{\max}^2} \tag{7}$$

3. Results

3.1. Mechanical tests

Table I lists values of the yield stress as a function of strain rate and test temperature. The Cross Bow system ($\dot{\varepsilon} \approx 10^4$) did not have the facility for testing other than at room temperature. The large increase in yield stress at high strain rates and temperatures below T_G is evident from the data. The flow stresses at 10% and 20% strain showed a similar pattern. Table II contains the values of the temperature rise for the strain limited tests. Fig. 1 depicts the temperature rise data. The four set of data can be fitted to fairly straight lines which supports Chou *et al*. [21] who suggested that the temperature rise may be assumed to be linearly related to the strain after the specimen yielded. Chou reported rises of 10 to 20 K at 20% strain and 10^3 s^{-1}, which are larger than the values tabulated in Table II for 30% strain.

TABLE I Variation of PET yield stress (MPa) with strain rate and temperature

	Temperature				
Rate (s^{-1})	263 K	298 K	323 K	363 K	453 K
0.001	68 ± 2	64 ± 2	29 ± 2	-	-
1200	130 ± 13	138 ± 20	138 ± 18	66 ± 9	42 ± 6
1900	165 ± 18	163 ± 23	160 ± 19	78 ± 9	42 ± 8
8800		204 ± 2			

TABLE II Calculated temperature rise values with strain and strain rate

	Temperature Rise (K ± 2)			
Strain (%)	10^{-3} s^{-1}	1 s^{-1}	1200 s^{-1}	8800 s^{-1}
30	9	12	9	
70	25	30	35	55
140	48	58	71	125
185	64	94	107	152

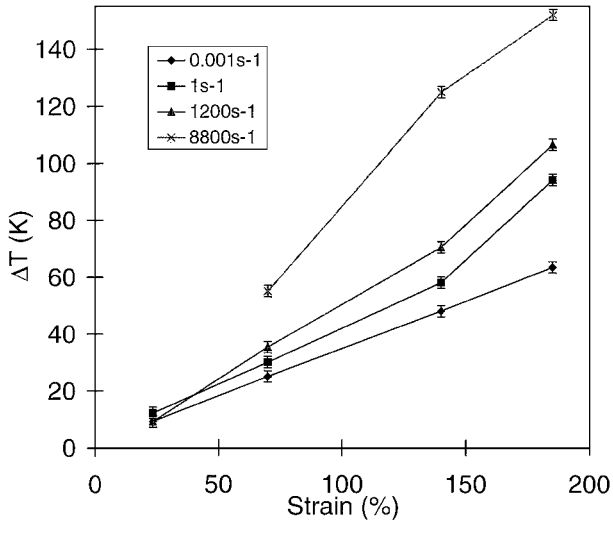

Figure 1 Temperature rise versus strain at different strain rates.

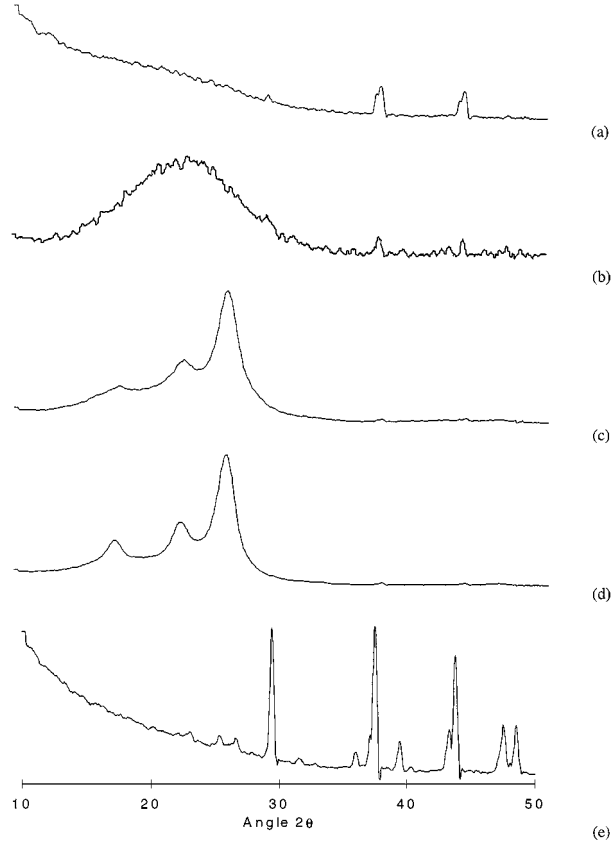

Figure 2 X-ray diffraction patterns of PET tested at 298 K: (a) undrawn; (b) 10^{-3}; (c) 1200; (d) 1900; (e) 8800 s^{-1}.

3.2. X-ray diffraction

The wide angle x-ray diffraction patterns of PET samples, as-received and tested at 298 K, at different strain rates are shown in Fig. 2. The as-received material appeared to be amorphous and isotropic. Compression at a slow rate oriented the material although diffraction peaks were not detected. The sharp peaks at 28°, 37° and 45° are due to the aluminium holder. At higher strain rates, 10^3 s^{-1}, three clear peaks were detected whose positions are in agreement with reported *d* spacing values for crystalline PET [4]. At the highest strain rate the pattern did not show diffraction peaks. On annealing, the untested as-received material orients, and shows three broad peaks when the annealing temperature exceeds the cold crystallisation temperature. When tested at 10^{-3} s^{-1} at 363 K, diffraction peaks due to crystals appeared, although they are very ill defined. This contrasts with the very intense peaks detected when samples are compressed at 453 K at this low strain rate. At strain rates in the 10^3 s^{-1} range, crystallographic peaks were detected in all the samples independently of the test temperature although samples tested below room temperature showed a less perfect structure. Fig. 3 shows the x-ray patterns of samples tested at different strain rates when the test was halted at 185% strain. It is clear that the crystalline development is only evident at the highest strain rates. At 10^{-3} and 1 s^{-1} only

TABLE III Variation of lattice spacing (Å) with strain rate and temperature

Rate (s^{-1})	T (K)	(0 1 0) ($\pm$0.02)	(1 1 0) ($\pm$0.02)	(1 0 0) ($\pm$0.02)
0.001	453	5.05	3.88	3.44
1200	298	5.03	3.94	3.44
1200	323	4.93	3.94	3.43
1200	363	5.05	3.97	3.47
1200	453	5.04	3.92	3.43
1900	263	-	3.95	3.45
1900	298	5.04	3.95	3.43
1900	323	5.05	3.95	3.44
1900	363	5.01	3.93	3.42
1900	453	5.04	3.92	3.41

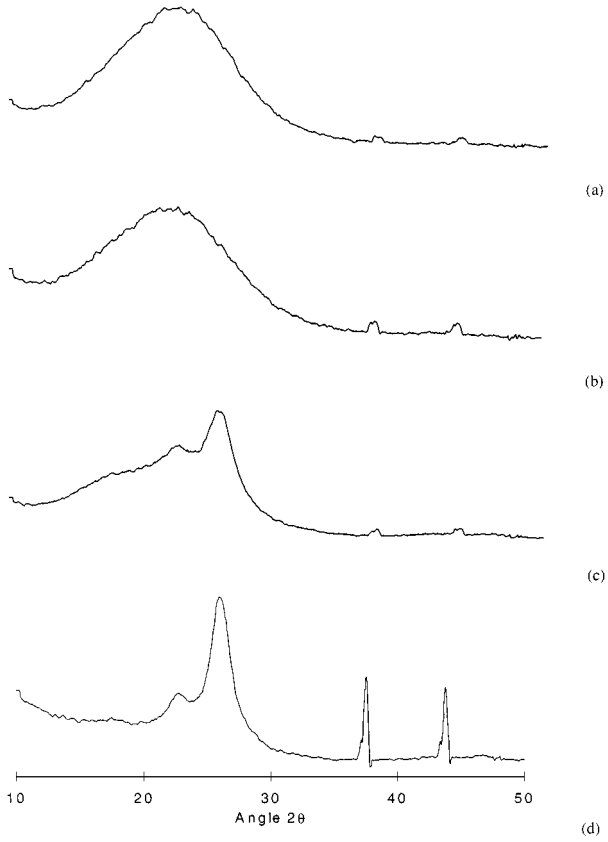

Figure 3 X-ray diffraction patterns of PET tested at 298 K up to 185% strain at: (a) 10^{-3}; (b) 1; (c) 1200; (d) 8800 s^{-1}.

orientation occurred after compression to any strain. However, samples tested at 1200 s^{-1} and 8800 s^{-1} showed evidence of orientation for strains up to 70% and evidence of crystal structure at higher strains.

The *d*-spacing values obtained from samples which gave rise to diffraction peaks are shown in Table III. The values found in compression are all below those reported by Jabarin [4]. Fig. 4 reveals that no major change occurred in the *d* spacing of a family of planes at a given strain rate when tested at different temperatures and that the *d* spacing values almost superimposed for a family of planes at different strain rates, indicating that there was no change in *d* with strain rate. This is in contrast to results obtained with PEEK which showed a drop in *d* spacing with strain rate [22]. Fig. 5 depicts the crystal size perpendicular to the (100) family calculated from Equation 2 and tabulated in Table IV. The

TABLE IV Variation of full width at half maximum and crystal size (nm) perpendicular to the (100) plane with strain rate and temperature

	Rate 1200 s^{-1}		Rate 1900 s^{-1}	
T (K)	FWHM ($\pm$0.05)	L (nm $\pm$ 0.1)	FWHM ($\pm$0.05)	L (nm $\pm$ 0.1)
298	1.49	6.05	1.56	5.83
323	1.47	6.18	1.45	6.25
363	1.52	5.96	1.09	8.29
453	1.46	6.22	1.13	8.06

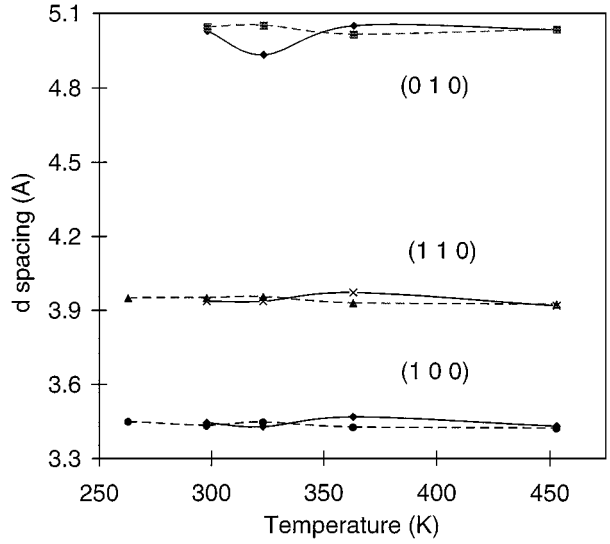

Figure 4 d Spacing versus temperature for the three main reflections. Continuous line 1200 s^{-1}; discontinous line, 1900 s^{-1}. Error bars are too small to be shown.

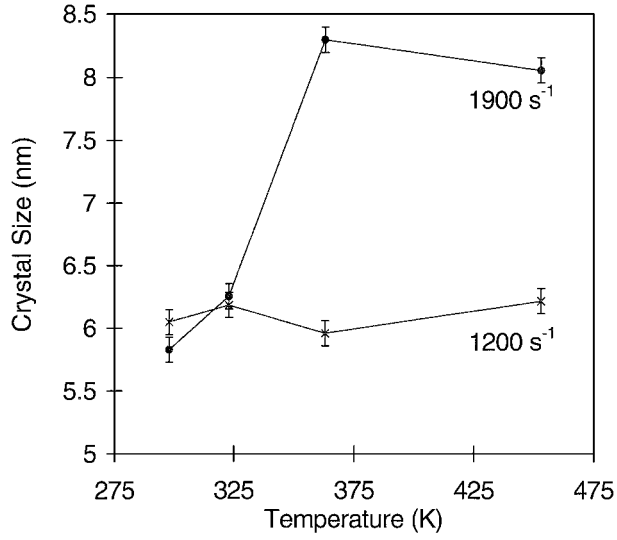

Figure 5 Crystal size versus temperature at different strain rates.

(100) peak was chosen for the calculations because it appeared in all the scans and, being the most intense, any change in crystallite size should be more easily detected than for the other peaks. It can be seen that up to test temperatures of around 323 K there is no change in crystal size with strain rate. At higher experimental temperatures the crystal size increased from 6 to 8 nm when tested at 1900 s^{-1}. The crystal size of samples tested at 453 K and 10^{-3} s^{-1} was approximately 4 nm.

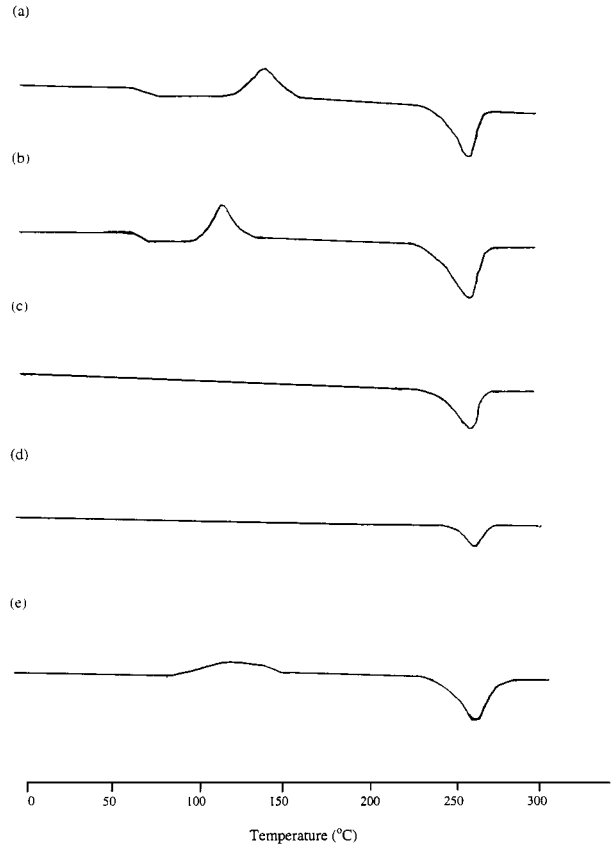

Figure 6 DSC scans of PET tested at 298 K at: (a) undrawn; (b) 10^{-3}; (c) 1200; (d) 1900; (e) 8800 s^{-1}.

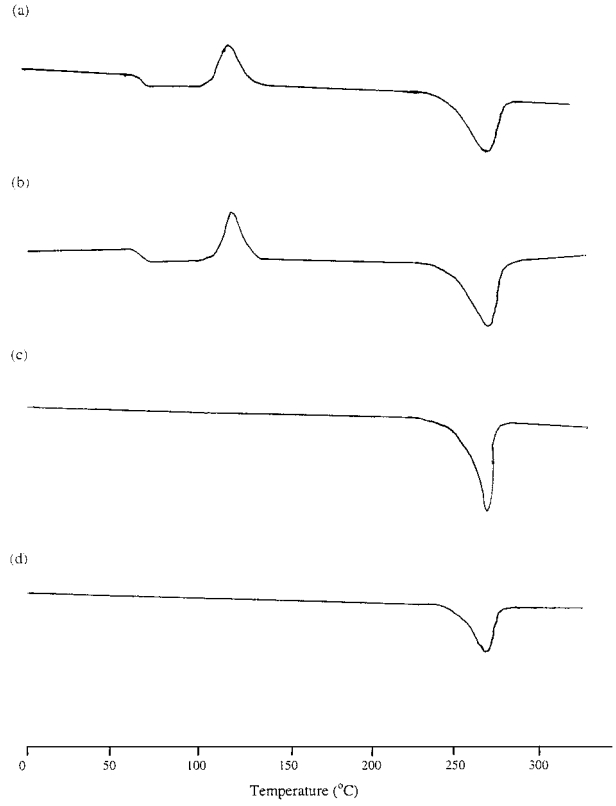

Figure 7 DSC scans of PET tested at 298 K up to 185% strain at: (a) 10^{-3}; (b) 1; (c) 1200; (d) 8800 s^{-1}.

3.3. Thermal analysis

The DSC scans of as-received PET and PET tested at different strain rates at room temperature are shown in Fig. 6. All DSC scans were performed at 10° min^{-1}. As-received PET underwent glass transition cold crystallisation and melting in the range 273–623 K. When compressed at low rates the thermal behaviour is very similar to as-received material with the glass transition and cold crystallisation very clear. When tested in the 10^3 s^{-1} range the glass transition and cold crystallisation are not visible in the scans. The cold crystallisation peak disappearance may be associated with a transition in physical properties such as density [23]. At 8800 s^{-1} the glass transition and cold crystallisation are very broad but clear. As-received PET underwent glass transition and cold crystallisation on annealing up to 363 K, when the peak occurred at about 415 K. When annealed at 453 K which is above the cold crystallisation temperature the material crystallised before the thermal scan and cold crystallisation was not seen. Under slow rate compression the thermograms are very similar to the as-received material, the glass transition and cold crystallisation very clear up to test temperatures of 363 K and absent at higher temperatures. The cold crystallisation peak temperature occurred approximately at 393 K. At 10^3 s^{-1}, there seems to be a transition in the material behaviour. The glass transition was not observed and the cold crystallisation represented a small percentage of the overall crystallinity content compared to the contribution of the melting endotherm. Samples tested at 1200 s^{-1} and 453 K and at 1900 s^{-1} at 363 K and 453 K showed a second small melting peak at a higher temperature. Fig. 7 shows the scans of samples tested up to 185% strain at different strain rates. It can be seen that the cold crystallisation and glass transition were not detected at the higher rates. At low rates, 10^{-3} and 1 s^{-1}, both transitions are clear up to 185% strain. Nevertheless, the cold crystallisation peak temperature decreased with strain from 418 K to 393 K and 415 K to 394 K respectively. At 1200 and 8800 s^{-1}, cold crystallisation is seen up to 140% strain, although it decreased in magnitude with strain and the peak temperature decreased from 414 K to 396 K.

The areas of the cold crystallisation peak and the heat of fusion for samples tested at different strain rates, temperatures and strains are tabulated in Tables V and VI while the overall crystallinity content obtained by subtracting the two previous values and dividing by 115 J g^{-1} is shown in Tables VII and VIII. Crystallinity content data are depicted in Fig. 8. The degree of crystallinity tended to increase with strain rate up to 1900 s^{-1} at any test temperature except 453 K when nearly all the crystallisation occurred before the

TABLE V Variation of cold crystallisation and melting endotherm with strain rate and temperature

	Cold Crystallisation/Heat of Fusion (J/g)				
Rate (s^{-1})	263 K	298 K	323 K	363 K	453 K
0	39/54	39/52	40/53	33/53	0/54
0.001	34/53	38/56	39/55	18/60	0/59
1200	21/54	8/58	3/56	7/55	0/57
1900	7.0/54	2/61	0/58	5/61	0/57
8800		25/54			

TABLE VI Variation of cold crystallisation and melting endotherm with strain and strain rate at 298 K

	Cold Crystallisation/Heat of Fusion (J/g)			
Rate (s^{-1})	30% strain	70% strain	140% strain	185% strain
0.001	39/53	38/52	36/54	34/55
1	37/51	37/54	32/53	33/53
1200	37/53	37/52	32/54	0/58
8800		37/53	23/55	2/56

TABLE VII Variation of crystallinity content (%) with strain rate and temperature

	Crystallinity Content (% ± 1)				
Rate (s^{-1})	263 K	298 K	323 K	363 K	453 K
0	13	12	12	18	47
0.001	16	16	14	37	51
1200	29	44	46	42	50
1900	41	52	50	48	50
8800		25			

TABLE VIII Variation of crystallinity content (%) with strain and strain rate at 298 K

	Crystallinity Content (±1)			
Rate (s^{-1})	30% strain	70% strain	140% strain	185% strain
0.001	13	13	16	19
1	12	14	18	18
1200	14	13	19	50
8800		13	28	47

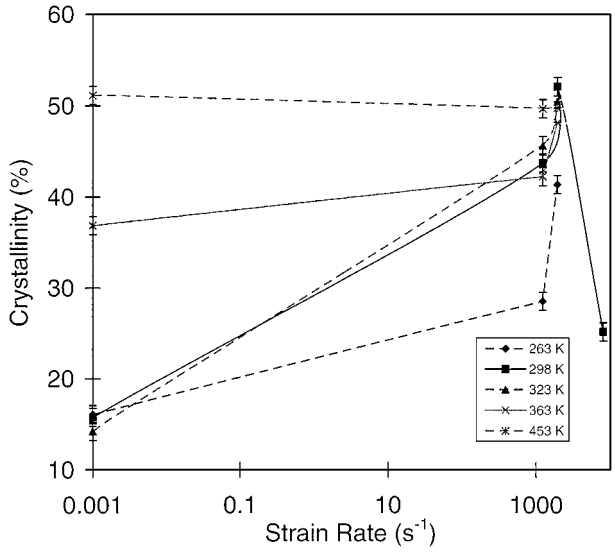

Figure 8 Crystallinity content versus strain rate on a logarithmic scale.

compression began. Samples tested at low strain rates needed higher test temperatures to reach a high degree of crystallinity. Fig. 9 show the crystallinity content of samples tested at different rates to different total strains. At low strain rates or small amount of strain the degree of crystallinity increased very little but large increases were found when compressed beyond 140% at rates above 10^3 s^{-1}.

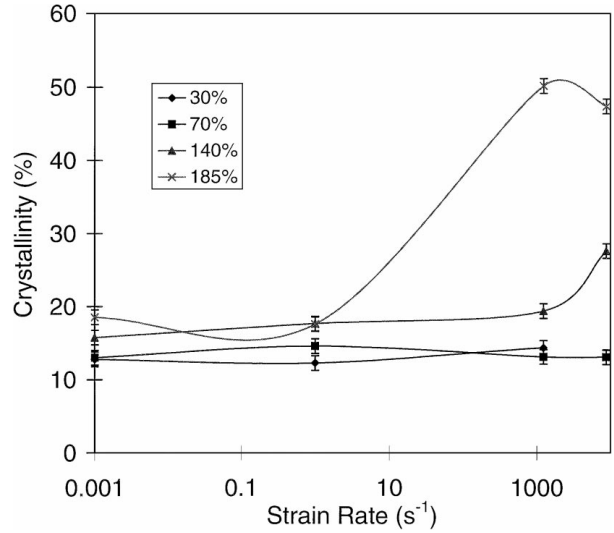

Figure 9 Crystallinity content versus strain rate on a logarithmic scale.

3.4. Kinetics of crystallisation

The evidence presented in the above sections suggests that crystallinity increases occur predominately at high strain rates and at strains in excess of 140%. High strain rate leads to increased yield and flow stresses (Table I) and since the process is adiabatic to large temperature rises, (Table II). These temperatures may be sufficient for cold crystallisation to take place in the normal thermally induced manner and offer an explanation of the crystallinity increases observed after a test. However, in order to test this hypothesis the kinetics of crystallisation must be known. Experiments were therefore carried out to determine the cold crystallisation kinetic parameters. Untested as-received samples were used for all these tests. A knowledge of these parameters, and the assumption that the same parameters can be used in high rate tests, can be used to estimate the crystallinity as a function of time during a test and hence determine if crystallinity induced in this manner can be responsible for flow stress increases.

Owing to the asymmetry of the cold crystallisation peak the activation energy and pre-exponential factor were calculated following the methods outlined above using two different sets of peak temperatures. The cold crystallisation peaks temperatures can be seen in Table IX. Figs 10 and 11 show the fit of the data to the Kissinger and Ozawa methods. Average parameters were calculated from both methods. The low temperature peak temperatures yielded and activation energy for crystallisation of 117 kJ $mole^{-1}$ and a pre-exponential factor of 1.2×10^{15} min^{-1}. The high temperature peak gave 95 kJ $mole^{-1}$ and 2.5×10^{11} min^{-1}.

TABLE IX Variation of the cold crystallisation peak position with heating rate

RATE (K/min)	FIRST PEAK (K)	SECOND PEAK (K)
1	383.0	399.4
2	387.3	405.6
5	394.5	416.9
10	405.5	428.9
20	414.8	443.6

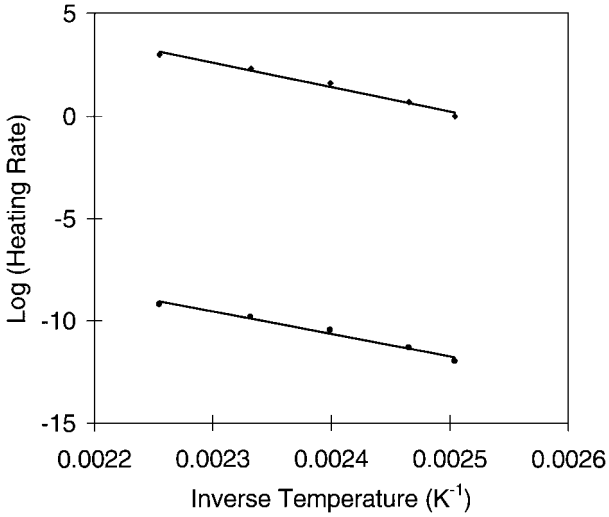

Figure 10 High temperature peak.Top: linear fit by Ozawa's method. Bottom: linear fit by Kissinger's method.

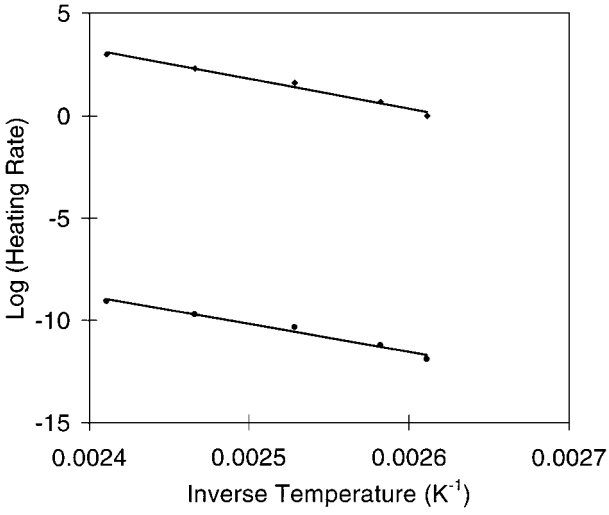

Figure 11 Low temperature peak Top: linear fit by Ozawa's method. Bottom: linear fit by Kissinger's method.

Sun *et al.* [24] reported activation energies of crystallisation of undrawn PET from their own experiments and others between 155 and 264 kJ mole^{-1}. The present values are smaller than the previous values but are larger than the value of 84 kJ mole^{-1} reported by Cobbs and Burton [25].

During a high rate compression test the temperature of the sample rises by 100 K in approximately 1.3 ms. It is estimated that the sample reaches the temperature for onset of crystallisation, about 373 K, approximately 1 ms after the compression begins, that is to say when the temperature increase is about 80 K. Thus, cold crystallisation may have happened during the last 0.3 ms of a test, this prediction is backed up by the evidence from the strain limited tests. Assuming that the temperature is 373 and α, the degree of conversion, is equal to 0 at the temperature at which cold crystallisation commences, an increase in α over a period of 0.3 ms was calculated using Equation 4 rearranged:

$$d\alpha = kg(\alpha)\, dt$$

The calculation was carried out under the assumption that the temperature was constant since a single value of

TABLE X Increment in the degree of conversion, α, at 373 K after 0.3 ms. Middle column, $E = 117$ kJ mole^{-1}, $A = 1.2 \times 10^{15}$ min^{-1}. Right column, $E = 95$ kJ mole^{-1}, $A = 2.5 \times 10^{11}$ min^{-1}

$g(\alpha)$	$d\alpha_1$	$d\alpha_2$
1-α	2.2×10^{-7}	5.9×10^{-8}
2 (1-α)$^{1/2}$	4.4×10^{-7}	1.2×10^{-7}
3 (1-α)$^{2/3}$	6.6×10^{-7}	1.8×10^{-7}

TABLE XI Increment in the degree of conversion, α, at 405 K after 4 s. Middle column, $E = 117$ kJ mole^{-1}, $A = 1.2 \times 10^{15}$ min^{-1}. Right column, $E = 95$ kJ mole^{-1}, $A = 2.5 \times 10^{11}$ min^{-1}

$g(\alpha)$	$d\alpha_1$	$d\alpha_2$
1-α	0.05	8.9×10^{-3}
2 (1-α)$^{1/2}$	0.10	0.02
3 (1-α)$^{2/3}$	0.15	0.03

the rate constant, k, was used. The value calculated can be interpreted as the isothermal increase in α in 0.3 ms. It is reasonable to conclude that the values obtained are an underestimation since at higher temperatures α can only increase. Table X summarises the results for several $g(\alpha)$ forms. The results show that no significant amount of crystallisation occurs during a compression test due to the temperature rise alone. When the end of a typical high rate compression test was reached the sample temperature was at least 405 K. The sample then cooled down slowly. By drilling a small hole in a sample and inserting a thermocouple into the hole the time taken for a PET sample to cool from 405 K to 373 K when the sample was between two steel rollers (simulating the situation in a high rate test) was found to be 4 s. Calculations were carried out which are tabulated in Table XI to determine the amount of crystallisation likely to occur in this cool down period. It can be seen that the degree of conversion ranges from 1 to 15%. It must be borne in mind that at 405 K the rate of crystallisation of PET is low.

4. Discussion

As-received PET was probably an isotropic material consisting of two phases- a small quantity of crystalline phase, about 10% as determined by thermal analysis, randomly dispersed in the prevailing amorphous matrix. Since the material was received in plaque form, it is very likely that the chains run more or less parallel to the plaque surfaces. The history of the material is not known but it seems that it was rapidly quenched from the melt. The amorphous phase was probably highly entangled but the chains were in a more or less extended configuration because of the difficulty that PET has in forming folded structures compared to other polymers with a much more flexible chain. PET presents two conformational isomers, namely trans and gauche, which arise from the different positions that the glycol group can assume. The gauche conformation is found only in the amorphous regions as it cannot occupy normal lattice positions whereas the trans form can exit in both amorphous and crystalline regions. The growth of the

crystalline structure occurs by addition of material to nuclei to form crystallites. Nuclei are formed as a result of thermal fluctuations [26] or already exist in the melt and are frozen during quenching. The availability of nuclei is essential for posterior growth of crystals. Orientation of the amorphous phase occurs by chain slippage, configurational change, C-H wagging vibration and aromatic C-H bending mode, conformational change also contributes to the overall orientation as described by Dulmage and Geddes [27].

Low strain rate tests are isothermal in nature. Although the temperature rise estimated from the stress strain data was as high as 65 K, no sizeable temperature rises occur since this calculation is based on the assumption of an adiabatic process and the time required to dissipate heat is much smaller than the characteristic time of the low rate experiments. Thus, the small but real increase in crystallinity content detected on samples tested below the glass transition cannot be due to thermally induced cold crystallisation but must be real strain induced crystallisation. Thus, small crystals were formed by correct juxtaposition of chains into already existing nuclei. However, the rate of relaxation of chains as they slipped past each other may have exceeded the rate of strain induced nucleation and this avoided heavy nucleation and prevented a large increase in crystallinity. At test temperatures above the glass transition crystallisation happened before deformation started. When tested at low rates at 363 K a further increase in crystallinity of 19% occurred during deformation. Again, owing to the isothermal conditions it must be pure strain induced crystallisation. The crystals formed before the deformation started acted as nuclei and grew as the compression proceeded. For tests carried out at 453 K the crystallinity did not increase as a result of deformation, but, it seems that the crystals were more perfected and/or larger when compared with the annealed as-received material. This perfectioning process can occur by the pulling of defects out of the crystallites into the amorphous phase.

Previous workers have reported large amounts of strain induced crystallisation at low rate of straining even below the glass transition temperature. Nevertheless, it is clear from Tables VII and VIII that the increase in crystallinity content is very small in the tests reported here. The orientation of the amorphous phase plays a very important role in crystallisation. In tension, the test arrangement favours the orientation of chains in the direction parallel to the acting stress. The orientation as the deformation proceeds, reduces the conformational and configurational entropy, conditions needed for crystallisation to occur. The crystals formed are of fibrillar type. However, under a compression load the sample is allowed to expand in two directions perpendicular to the applied stress. The three crystallographic planes formed by PET are parallel to the z axis, and thus, it can be concluded that the molecules stack in the x and y planes with the chain axis parallel to the z direction. These chains, which are perpendicular to the stress, can adopt any direction in the plane of the sample. So, crystallisation occurs but probably only in small regions where the chains are aligned correctly. It seems that the likelihood of chains being properly brought together by the stress is greater in tension than in compression.

Tests at or above 10 s^{-1} proceeded under adiabatic conditions. The heat developed increases the temperature of the sample in accordance with the temperature rise estimates. The question arising is why low strain rates brought about a small crystallinity content increase while higher strain rates induced a large amount of crystallisation. The tests carried out in the 10^3 s^{-1} range at 263 K may provide information in this area. These tests showed that the crystallinity content was smaller than in samples tested at higher temperature, cold crystallisation was present and the structure formed was not very perfect. Strain softening is significant but the temperature attained in the sample during the test was some 30 K below that attained in the room temperature tests. Therefore, it seems that there is a direct correlation between the temperature reached in the sample and the increase in the crystallinity content.

The temperature for the induction of crystallisation under adiabatic conditions can be estimated from the strain limited tests. At 1200 s^{-1} crystal structure was seen to develop at strains of 140% with a crystallinity increase of 7% for a temperature increase of about 70 K. Therefore, it can be concluded that the structure developed and the crystallinity experienced a significant increase, above 5%, when the temperature rise was about 65–70 K, i.e. the temperature in the sample was approximately 363 K. However, some increase in crystallinity above that of the untested sample occurred a few degrees below this, and so it seems that under stress, crystallisation begins to take place at temperatures just above the glass transition temperature, but at a very small rate.

The sharp glass transition shown by the as-received material was not perceptible in the thermograms of samples tested at 10^3 s^{-1}. The glass transition is determined by movement in the amorphous phase, thus, the absence of the transition was probably due to physical crosslinks induced by the crystalline entities. The cold crystallisation peak decrease can be related to the reduction of entropy with preferential orientation [16]. Thus, specimens which did not crystallise at any stage, i.e., showed a large cold crystallisation peak, were oriented by the compression and the molecular chains required a lower energy to be crystallised.

The crystal size perpendicular to the (100) direction increased from 6 to 8 nm in samples tested above the glass transition temperature. This increase was accompanied by a second small melting peak at a higher temperature. The origin of this peak is not clear but it definitely has a true microstructural origin and it could be due to melting of small domains containing larger and more perfect crystals.

Samples tested at 8800 s^{-1} showed a lower degree of crystallinity than samples tested in the 10^3 s^{-1} range. Temperatures near the onset of melting were attained in the Cross Bow system since the final strains could not be limited and were probably larger than 185%. This eliminated any trace of crystals or nuclei present in the sample before the test. As-received PET quenched from

the melt under an N_2 atmosphere gave a crystallinity content of 23% and a DSC trace similar to samples tested at 8800 s^{-1}. Thus, it is highly likely that those samples tested in the Cross Bow reached the melting temperature and then re-crystallised during cooling and the crystallisation evolved in a similar manner to samples quenched from the melt.

It seems that the increase in yield stress found at medium-high strain rates cannot be related to the high degree of crystallinity detected in samples tested at high strain rates. Strain limited tests showed that crystallisation was induced only when samples were compressed to at least 140% strain. Kinetic estimations showed that crystallisation occurred when the test came to an end although not all the crystallinity increase could be accounted for in this manner. Two factors may account for a larger increase during cooling: i) the temperature rises were based on limited tests up to 185%, but it is almost certain that samples tested without constraints attained larger strains, which in turn yields higher temperature rises. Higher sample temperatures certainly means that more crystals were formed as the rate of growth of crystals in PET increases with temperature, reaching its maximum at approximately 450 K. ii) Kinetic parameters were calculated using isotropic samples, however, crystallisation in the sample started when it was oriented reducing the energy barrier to be surmounted. Therefore, a smaller activation energy would lead to a higher conversion factor, α, in the calculations. Moreover, the onset of crystallisation for oriented samples occurs in the order of milliseconds [26]. Thus, it is believed that the time scale of tests conducted at medium and above strain rates is too small for sizeable amounts of crystallisation to take place during the test and it must occur afterwards. The fact that the *d* spacing was almost independent of strain rate also supports this argument. Stress can cause a shift in the interatomic distances, however the crystal structure formed in the present samples did not depend upon the test conditions and is therefore likely to have been dominated by processes occurring after the removal of the stress.

However, it is remarkable that the crystallinity content up to the glass transition followed an approximately linear relationship with yield stress, see Fig. 12. A previous investigation on the yield stress drop at high strain rates showed that the trend of yield stress and crystallinity with strain rate were the same [28]. Therefore, the stress seems to be related to the structure induced afterwards. It may be that crystallisation is initiated by a critical stress level which may be established within the PET when the strain rate exceeded some critical values, and this is more important than the strain. Large strains did not induce crystallisation unless the strain rate was high. Strain rate plays an important role because the increase in yield and flow stress is a direct consequence of the increase in strain rate. Thus, the adiabatic conditions imposed by the strain rate and the strain rate exceeding the molecular relaxation rate lowered the barrier for crystallisation, heavy nucleation occurred and crystallisation took place to a large extent. Amongst all the processes involved in the deformation, it seems to be compulsory that a gauche-trans transition occurred in order to account for a large degree of crystallisation. It can be argued that the conformational changes started at yielding.

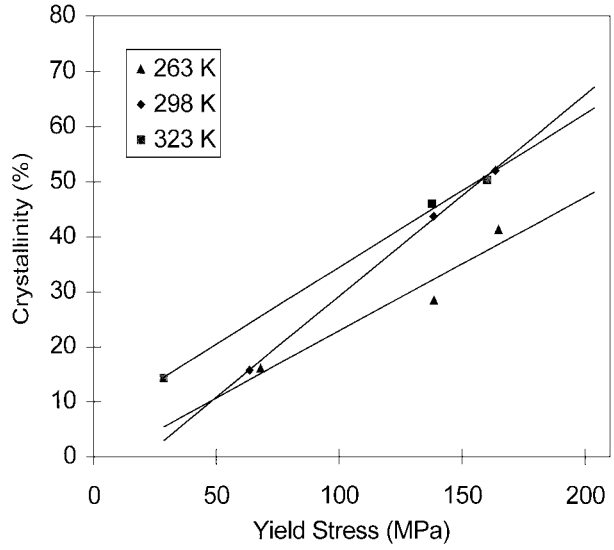

Figure 12 Crystallinity content versus yield stress.

5. Conclusions

Polyethylene Terephthalate showed three distinct crystallisation behaviours depending upon the strain rate:

i) Low strain rate, 10^{-3} s^{-1}. Temperature below the glass transition: the degree of crystallinity increased by a small amount when compared with undrawn material. The glass transition and cold crystallisation are clearly seen in the DSC thermograms. The strain induced crystallisation occurred during the deformation process which lasted for several minutes. However, the relaxation of chains and the lack of trans isomers prevented the formation of a large number of crystals and the final crystallinity content was small. Above the glass transition, crystallisation happened before the test started which favoured a further increase during testing.

ii) High strain rates, 10^3 s^{-1}. A large increase in crystallinity occurred, being smaller when the test temperature was below ambient. It is believed that thermally induced crystallisation took place after the compression was completed at these strain rates since it is very likely that it needed times of the order of seconds to be completed. A strain of at least 140% was needed to induce crystallisation and larger strains were required to induce increases of 30%. Isomerisation of the glycol group had to occur to account for such an increases. Strain induced crystallisation did not occur in the ms time scale of the tests.

iii) Very high strain rate, 9×10^3 s^{-1}. At this rate the time scale of the experiment is shorter than in case ii). Thus, crystallisation also occurred after the test came to an end. Strains above 140% induced a high final crystallinity content. However, tests without constraints gave a crystallinity content of about 25%. Since it is argued that crystallisation occurred after the test it cannot be argued that structure was formed as the strain was imposed and then destroyed. Therefore, the high

temperatures attained seem to be the only factor which may account for such a small crystallinity value. Melting or disruption of nuclei due to high temperatures in the sample probably gave rise to a similar crystallisation as that observed in rapidly quenched crystallisation from the melt.

Acknowledgements

The authors wish to acknowledge financial support from the UK Engineering and Physical Sciences Research Council under Grant GR/L14220.

References

1. DAUBENY, C. W. BUNN and C. J. BROWN, *Proc. Royal Society Series A* **226** (1954) 531.
2. A. MISRA and R. S. STEIN, *Journal of Polymer Science Part B* **17** (1979) 235.
3. J. E. SPRUIELL, D. E. MCCORD and R. A. BEUERLEIN, *Transactions of the Society of Rheology* **16**(3) (1972) 535.
4. S. A. JABARIN, *Polymer Engineering and Science* **32** (1992) 1341.
5. J. R. C. PEREIRA and R. S. PORTER, *Journal of Polymer Science Part B* **21** (1983) 1147.
6. L. Z. PILLON and J. LARA, *Polymer Engineering and Science* **27** (1987) 984.
7. D. J. BLUNDELL and B. N. OSBORN, *Polymer* **24** (1983) 953.
8. A. J. MULLER, J. L. FEIJOO, M. E. ALVAREZ and A. C. FEBLES, *Polymer Engineering and Science* **27** (1987) 796.
9. R. NATALE, R. RUSSO and V. VITTORIA, *Journal of Materials Science* **27** (1992) 4350.
10. N. ALBEROLA, M. FUGIER, D. PETIT and B. FILLON, *ibid.* **30** (1995) 1187.
11. S. M. WALLEY and J. E. FIELD, *Dymat Journal* **1** (1994) 211.
12. S. HAMDAN and G. M. SWALLOWE, *Journal of Materials Science* **21** (1996) 1415.
13. G. M. SWALLOWE, J. O. FERNANDEZ and S. HAMDAN, *Journal Phys. IV France* **7** (1997) C3:453.
14. D. J. BLUNDELL, D. H. MACKERRON, W. FULLER, A. MAHENDRASINGAM, C. MARTIN, R. J. OLDMAN, R. J. RULE and C. RIEKEL, *Polymer* **37** (1996) 3303.
15. S. HAMDAN and G. M. SWALLOWE, *Meas. Sci. and Technol.* **7** (1996) 1068.
16. M. CAKMAK and J. C. KIM, *Journal of Applied Polymer Science* **64** (1997) 729.
17. L. MANDELKERN, "Crystallisation of Polymers," (McGraw-Hill, US, 1964) p. 120.
18. H. E. KISSINGER, *Analytical Chemistry* **29** (1957) 1702.
19. T. OZAWA, *Bulletin of the Society of Japan* **38**(11) (1965) 1881.
20. R. N. ROGERS and L. C. SMITH, *Analytical Chemistry* **39** (1967) 1024.
21. S. C. CHOU, K. D. ROBERTSON and J. H. RAINEY, *Exp. Mechanics* **13** (1973) 422.
22. S. HAMDAN and G. M. SWALLOWE, *Journal of Polymer Science B Polymer Physics* **34** (1996) 699.
23. S. W. LIN and J. L. KOENIG, *Journal of Polymer Science: Polymer Symposium* **71** (1984) 121.
24. T. SUN, J. PEREIRA and R. S. PORTER, *Journal of Polymer Science Part B* **22** (1984) 1163.
25. W. H. COBBS and R. L. BURTON, *Journal of Polymer Science* **10** (1953) 275.
26. F. S. SMITH and R. D. STEWARD, *Polymer* **15** (1974) 283.
27. W. J. DULMAGE and A. L. GEDDES, *Journal of Polymer Science* **31** (1958) 499.
28. N. AL-MALIKY, J. O. FERNANDEZ, D. J. PARRY and G. M. SWALLOWE, *Journal Materials Science Letters* **17** (1998) 1141.

Received 11 May 1999
and accepted 1 February 2000